Th. Wuebben, J. Banhart, S. Odenbach

Production of Metallic Foam under Low Gravity Conditions during Parabolic Flights

Metallic foams are a recently developed light weight material. They are porous structures consistent of metals like aluminum, tin, zinc, lead etc. or their alloys. The pore sizes are in the range of millimeters and relative densities down to 10% of the original material can be achieved.
Since metallic foams combine relative low weight with high stiffness, their applications are mainly for means of light weight structures as used for example in cars. Also other applications like sandwich structures and metallic filters are of interest.
To make metallic foams applicable for an industrial use, still some technical and principle problems have to be solved. These concern mostly the structure of the resulting foam, which is very inhomogeneous and not well understood.
Our aim is to contribute to the understanding of the physical processes that take place during the foaming process. In this paper we will introduce the powder metallurgical production method we used for producing metallic foams. Then we will describe the two main physical processes during the foam genesis and present our experimental idea and setup used to obtain information on these processes. Finally we will discuss the first results we got from parabolic flights and terrestrial experiments.

1 Powder metallurgical production process for metallic foams

The precursor material we used for our investigations was produced in a powder metallurgical process as described schematically in the pictures below (Fig. 1):
in a first step, the metal powder and the propellant or so-called blowing agent are well mixed in a ball mill (see Fig. 1a). The type of propellant mainly depends on the melting point of the used metal. The mixture is then compacted or extruded (Fig. 1b). This leads to a foamable material, which can be worked on to obtain a customized shape of precursor material (Fig. 1c). The metallic foam is then produced by melting this semi finished product (Fig. 1d): as soon as the metal becomes liquid, the propellant starts to expand in a chemical reaction and bubbles arise inside the melt. The cellular structure can be conserved by cooling down the metal under its solidification point.
Since the foaming process can be run inside a customizable mold, almost any desirable shape can be foamed, for example light weight structures as used in cars (see Fig. 2a). Additionally sandwich structures can be made by using appropriate mold materials (see Fig. 2b).
The melting temperature and duration of the foaming process have major influence on the resulting cellular structure, for example concerning density and homogeneity of cell sizes. Also process parameters like content of propellant inside the precursor material (which is in the order of a few

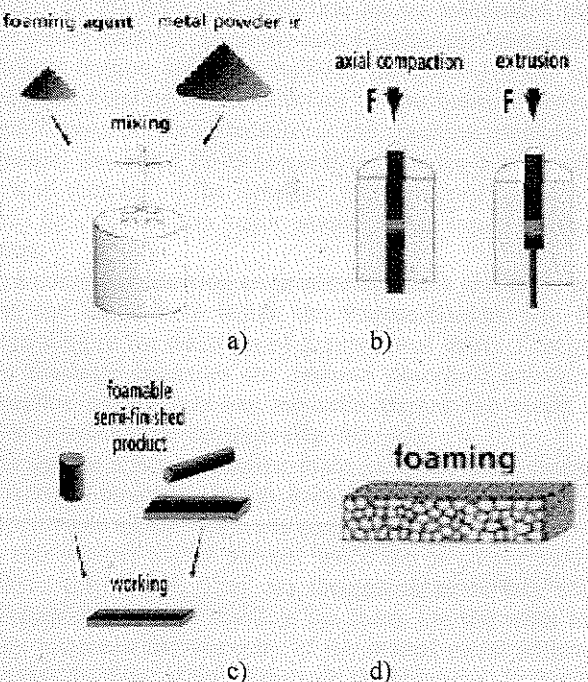

Fig. 1: Production process (for details see [1]).

weight percent) or the granular size of the powders affect the result.
In addition to this the physical processes during the evolution of the foam are not understood in detail. It is not clear which roles surface tension of the liquid metal and gravity driven drainage play and how they interact. This is the

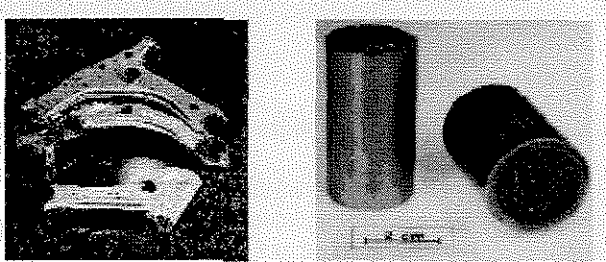

Fig. 2: Lightweight (a) and sandwich structures (b).

subject of our research. In the following we will describe the underlying physical phenomena in more detail.

2 Physical description of the foaming process

During the melting of the precursor material the expansion of the blowing agent leads to the formation of a metallic foam in various stages. These steps of foam genesis take place in a non-equilibrium state of the melt and are thus not sharply separable. Nevertheless one can distinguish four phases the melt undergoes before it is cooled down to solidification. The steps of foam formation as we understand them are depicted in fig.Fig. 3a)-d).

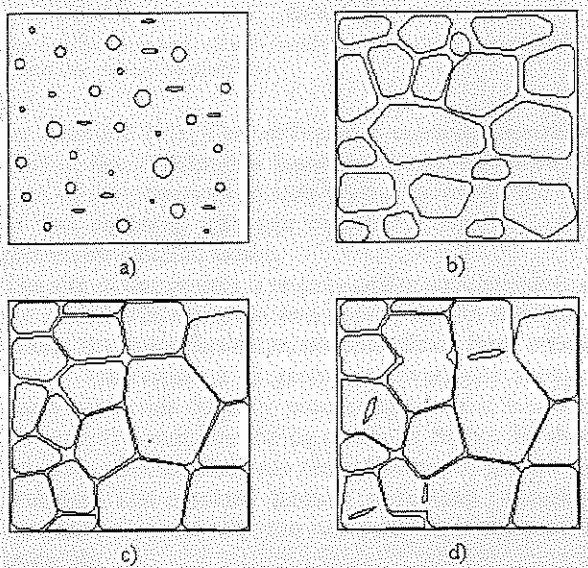

Fig. 3 : Four steps of foam genesis: a) start of foam genesis; b) young foam; c) completed foam; d) coarsened foam

At the very beginning, the material is solid and the propellant can't set free its gas. As the temperature increases, the material softens and small bubbles and distortions appear (Fig. 3a). These pores are generally of spherical shape since at this stage they don't interact with each other. However, due to the forces applied during the production process (step 2, fig. Fig. 1b), there will be a number of non-spherical but rather elliptical pores as well.

When the whole sample is in a liquid condition, the gas set free in a chemical process by the blowing agent can expand and the pores start to grow (fig. Fig. 3b). In this stage of a so-called young foam we have a two-phase system of gas and liquid metal. Thus the melt is undergoing a change from a wet foam (high liquid content compared to gas volume) to a dry foam (low liquid content). This in turn is accompanied by a change of pore shapes: during the growth the former individual bubbles start to interact with each other and undergo a metamorphosis from spherical to polyhedral cells of distributed sizes (fig. Fig. 3c).

However, if one analyses a solidified metallic foam one sees a coarse structure and ruptured cells. Also X-ray observations reveal a much more complicated scenario of foam evolution [2]. This can be explained by having a closer look into the two-phase system. In fig. Fig. 4 the

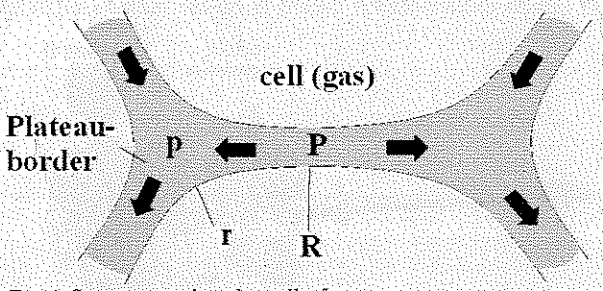

Fig. 4: Situation in a liquid metallic foam

region between gas filled cells and surrounding liquid is shown. This region is built up by the lamellae, which separate two cells and the Plateau-borders at the junctions of four cells. The interface between liquid metal and gaseous cells is characterized by the surface tension γ. γ itself depends on the presence of surface active substances inside the liquid material. These so-called surfactants decrease the surface tension and thus stabilize the cells. On the other hand the bending of the interface differs between lamellae and Plateau-borders. Because of the resulting pressure difference, the liquid flows towards the Plateau-borders at the cost of thinning of the lamellae. The junctions between the cells thus contain the major amount of the liquid inside the foam.

In a normal production environment, where gravity is present, the liquid held within the Plateau-borders will flow according to the direction of gravitational force. This gravity drainage enhances the process described above: the lamellae will rupture and the cells merge. The result is a coarse structure of the foam (fig. Fig. 4d).

The longer a liquid metallic foam lasts, the more drainage affects its structure. It can even lead to a collapse of the foam, when all the liquid has drained out.

In this context oxides present inside the precursor material play a major role. They are thought to as surface active substances and thus stabilize the foam. On the other hand they influence the viscosity of the melted metal which increases the flow of liquid through the junctions. In fact first experiments with precursor materials having a lower than normal oxide content showed a much more unstable foaming process.

In figure Fig. 5 the expansion and following collapse of an Al foam is shown. After the temperature has reached the melting temperature of the sample, the expansion starts. It is followed by a clear observable collapse as the heating continues.

3 Aim of the project and experimental idea

As previously described surface tension and gravity driven drainage have major influence on the foaming process. For aqueous steady foams this has been investigated to a certain extent and led to the so-called foam drainage equation (see,

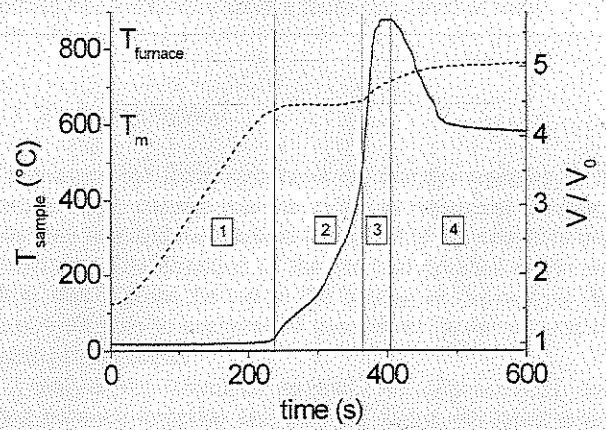

Fig. 5: Expansion and collapse (solid line) of an Al foam versus time; dotted line: furnace temperature

for example [3]). This differential equation describes the flow of liquid through a foam and meets well with the results of investigations at soap froths. However, the validity of this equation, although reasonable, has not yet been proved for metallic foams.

The aim of our project is to get a better understanding about the roles surface tension and gravity driven drainage play during the foam formation process. Since both effects are strictly correlated, it is useful to investigate them separately. This was done by processing metallic foams under low gravity conditions during parabolic flights. By doing so we were able to eliminate the influence of gravity driven drainage. The obtained samples were then compared to samples processed with the same experimental parameters in the lab.

In the following chapter we will describe the experimental set-up we used to perform our investigations.

4 Experimental set-up

In fact, there are some major differences in researching metallic foams compared to aqueous foams. First, metallic foams are always produced by melting a metal and then freezing the structure by solidification. The whole formation process takes place in an opaque system and thus cannot be easily observed optically. Additionally the high conductivity of the melt rules out resistance measurements as often applied in aqueous foam research ([4]). Other observation techniques are X-ray beams (to look into the foam) or laser expandometers (to observe volumetric parameters). But while the first requires facilities like a synchrotron at ESRF in Grenoble, the latter occupies too much space for being used on parabolic flights.

Because of the lack of appropriate observation techniques we focussed on building a device which allows us to produce metallic foams in a highly controllable way in the lab as well as on parabolic flights. The influence of gravity was then investigated by analyzing the resulting pore structures of the samples.

The experimental set-up is shown schematically in fig. Fig.

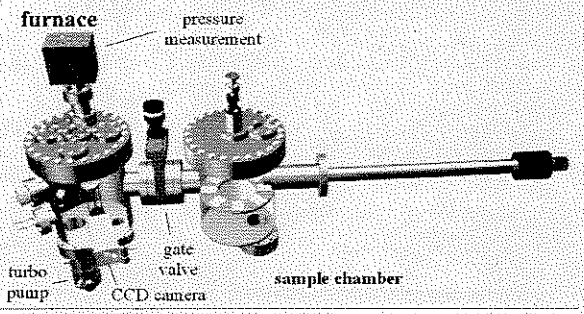

Fig. 6: Experimental set-up (schematically); overall length is approx. 2m.

6. It consists of two main parts: the furnace and the sample chamber. The furnace chamber is equipped with a temperature controlled heating jacket (not shown) to allow air temperatures up to 250°C. The samples are processed on a heating plate inside this chamber, which allows local temperatures of approx. 600°C. For the first campaigns it was driven by a heating wire system. But since this system was sensitive to technical failures it was replaced by an infrared light source.

The samples are of 20x20x1.8 mm³ in size and are held in appropriate containers. These sample holders allow for almost free foaming of the material, while the heating power is applied through the thin (0.5mm) copper bottom of the container.

To perform an experiment one sample container is mounted onto the heating plate in a way that the sample temperature can be measured by a thermocouple. A programmable temperature controller then provides different scenarios to apply to the sample. At the end of the process the structure is frozen by cooling down the melt with pressurized air.

During the process the temperatures of the sample and surrounding air are measured. The stage of foaming can be correlated to the measured temperatures by a video system.

The sample chamber (on the right in the picture) is needed for keeping the samples during parabolic flights. It is capable to store up to 12 samples in their containers. During flights the samples are transferred manually by a transfer bar into the furnace and placed on the heating plate. After completing the foaming process they are returned to the sample chamber again and the next sample is picked up.

5 Results

For our investigations we used lead alloys as precursor material. These are expected to be prone to gravity driven drainage because of their high densities. Although there are no specific advantages of lead foams for being used in an industrial way, we are convinced to use them as a model for other metallic foams. In fact they show the same foaming behaviour and general foam structure like for example aluminum foams. The low melting points of the used alloys (between 200°C and 300°C) on the other hand make the

performing of experiments much easier than that of other metals like aluminum from a technical point of view.

5.1 Analyzing method

To analyze the foam structures we cut the samples in the middle. The cutting was done by an electrical discharge machine to avoid mechanical treatment of the sensitive pore structures. The direction of the cut was parallel to the heat flow, that is from the top to the bottom of the sample. We thus were able to analyze the amount of liquid drained out during the process.
To analyze the structures optically we enhanced the contrast between lamellae and cells by filling the latter with a

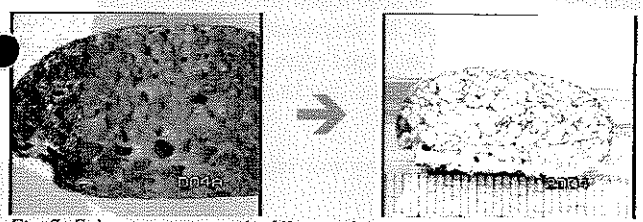

Fig. 7: Enhancing contrast by filling with creme

white substance, like creme or gypsum (see fig. Fig. 7).

In the next step the photographs of these structures were analyzed by a digital image processing software with regard to cell size and circularity (see fig.Fig. 9):

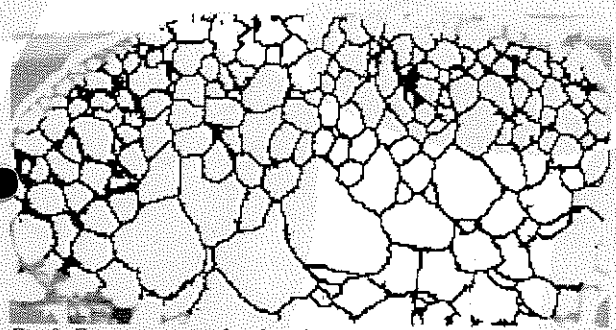

Fig. 9: Foam structure after digitalization (watershed separation)

the photographs are sharpened and the luminescence is adjusted. After removing the remaining ruptured lamellae, a watershed separation is a applied and the resulting areas are measured.

5.2 Comparison of foaming durations

In fig. Fig. 10 we present a comparison of two samples (material: PbSb10Sn10) which were heated for different times so that different stages of the foaming process are visible. Both samples were processed under normal g conditions.

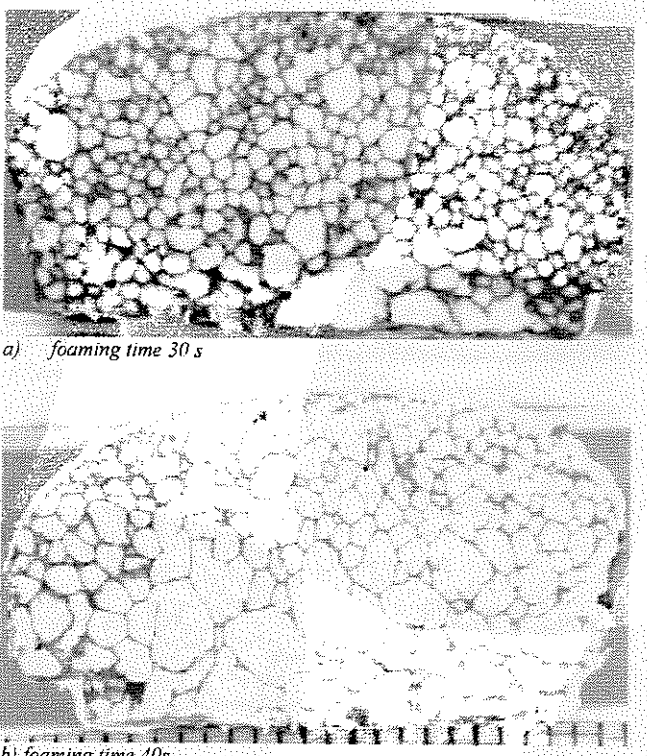

a) foaming time 30 s

b) foaming time 40s

Fig. 10: Comparison of different durations of foaming processes

While the upper one shows generally intact and rather small cells, the lower one exhibits the rupture of cells due to an advanced stage in foam formation.

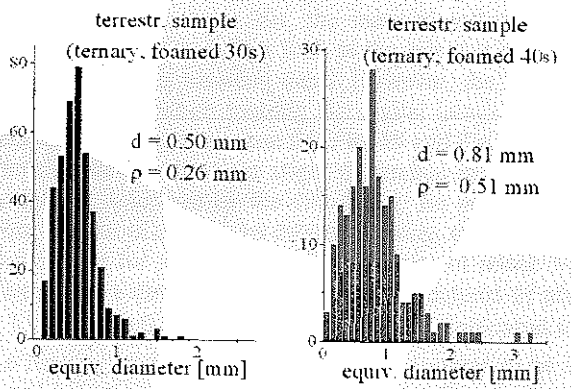

Fig. 8: Comparison of equivalent diameters for varied durations of foaming time (material: PbSb10Sn10); d indicates the mean average of equiv. diameters, ρ its standard deviation. The error is in the range of 0.02 mm for both.

This is proved by the results of the digital analysis of the structures (see fig. Fig. 8 and Fig. 11). In this context the equivalent diameter is defined as the diameter a circle of the same size like the cell under consideration would have. The circularity is defined as the square of the perimeter divided by the area of the pore. It measures the difference of the cell shape compared to a perfect circle. For simplicity it was divided by 4π in the present case (thus a perfect circle would have a circularity of 1).

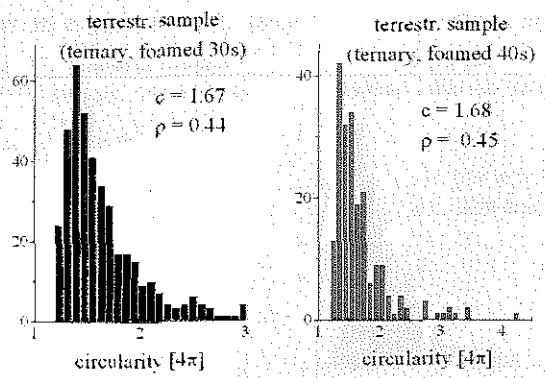

Fig. 11: Comparison of circularities for varied durations of foaming time (material: PbSb10Sn10); c is the mean average of circularities, ρ its standard deviation. The error is in the range of 0.01 for both.

The difference in the two cases is most obvious when analyzing the equivalent diameters of the cells. The longer duration of heating not only leads to increased cell sizes. Also a wider distribution of cell sizes is observable.

5.3 Samples foamed under low gravity conditions

In this section we will discuss the results of the first parabolic flight campaigns with ESA and DLR in October and December 1999. We were able to perform experiments with three different alloys: a lead tin alloy (PbSn30, melting point at $T_m \approx 200°C$), a lead antimony alloy (PbSb10, $T_m \approx 260°C$) and a ternary alloy of lead, tin and antimony (PbSb10Sn10, $T_m \approx 250°C$). However, at this stage only the latter one (the ternary alloy) has been analyzed because it showed the most homogeneous foam structure.

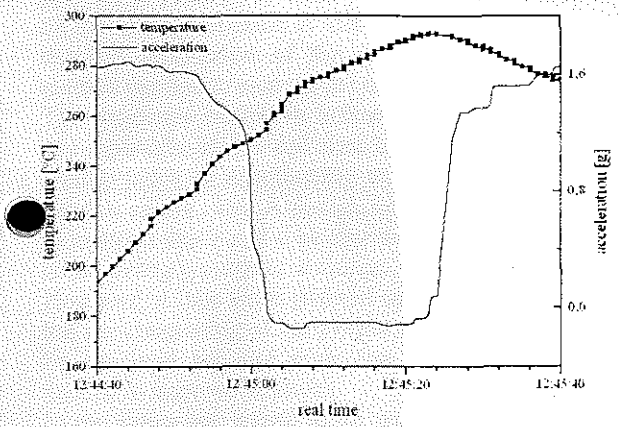

Fig. 13: Temperature and acceleration measurement for a ternary sample

In figure Fig. 13 the temperature and acceleration data of a ternary sample are plotted as an example. Since the sample temperature was measured only by a temperature sensor in contact with the surface of the sample, the melting point is only slightly visible ($T_m \approx 250°C$). The temperature curve was correlated with the video observation to ensure the foaming process (except the very beginning) took place during the low gravity phase. In the plot the cooling seems not to lead to an decrease of the temperature below the melting point. This has to be attributed to the fact that not only the sample but also the container holding the sample is warmed and thus affects the temperature measurement. In several tests we verified that the cooling system is able to freeze the structure in less than 3 seconds so that we are convinced the foaming process was stopped before entering the 2g-phase.

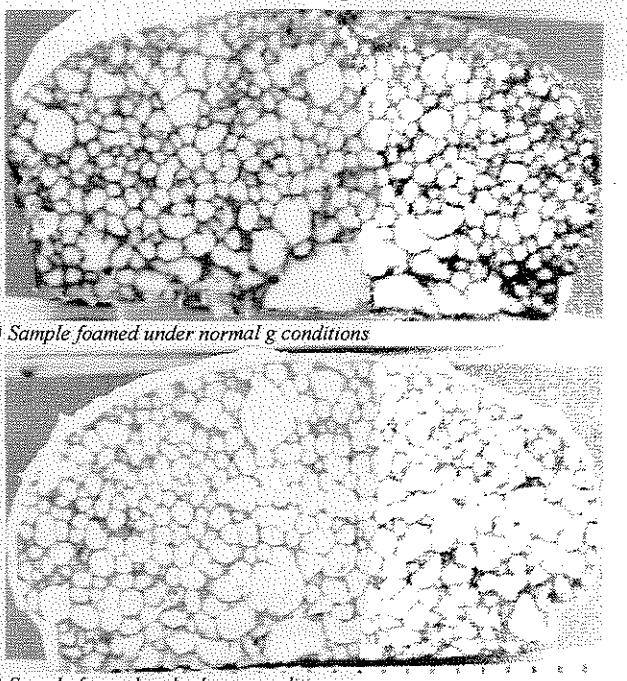

a) Sample foamed under normal g conditions

b) Sample foamed under low g conditions

Fig. 14: Comparison of sample foamed under normal and under low g conditions (material: PbSb10Sn10).

In figure Fig. 14 photographs of samples processed under different gravity conditions are shown. The foaming times for both samples were 30s, the material was the ternary alloy PbSb10Sn10. A first look at the samples shows only slight differences between them. However, the differences become visible when running the digital image processing over these photographs (see fig. Fig. 15 and Fig. 16).

The comparison shows a slight difference in the shape of the pores, described by the circularity: for samples underlying terrestrial conditions during foaming, the circularity is higher than for µg samples. The statistics of about 5 samples shows a circularity for terrestrial structures of about c = 1.7 ± 0.1 and a width of $\rho_c = 0.4 \pm 0.1$ compared to c = 1.6 for µg-samples. Thus the pore shape seems to be influenced by gravitational forces.

This is supported by the result of the analysing of the pore sizes: for terrestrial samples the pores are significantly larger (0.81 ± 0.03 mm) than for µg samples (0.6 mm). This

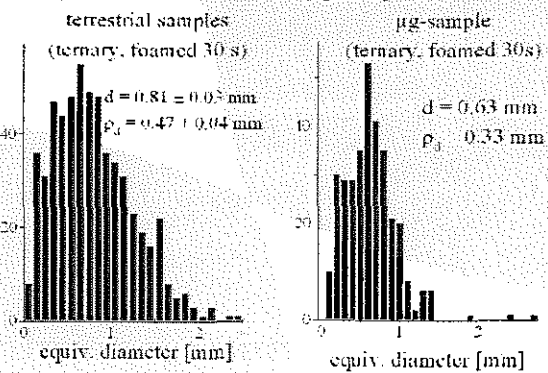

Fig. 15: Comparison of equivalent diameters for samples foamed under varied grvity conditions

was an expected result, since the gravity driven drainage

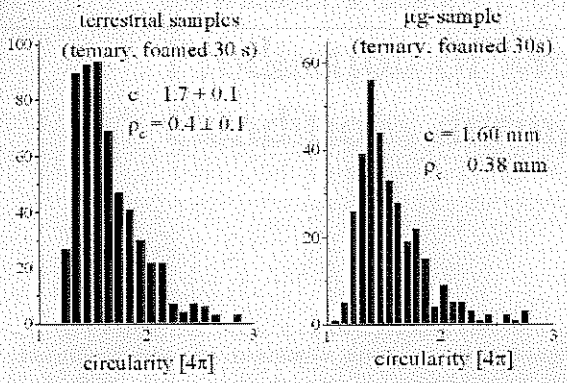

Fig. 16: Comparison of circularities for samples foamed under varied gravity conditions

enhances the film thinning due to surface tensional effects. Even though the material (PbSb10Sn10) shows only small visible drainage effects, the difference amounts to a factor of 1.3 in diameter.

Thus in total we can say that the gravitational conditions affect the size and the shape of the pores building up the foam.

6 Summary and outlook

In this article metallic foams as a modern material are in introduced. In way of discussing the physics underlying the production process, the influence of gravity driven drainage on the foam generation is discussed. This is followed by a detailed description of the experimental set-up and the method applied to analyze the obtained samples.

The structures exhibit an influence of gravity driven drainage especially on the cell size: an absence of gravity acceleration leads to significantly smaller mean equivalent diameters of the cells. Although this was to be expected, it is to mention that it could be shown even for a material which is not strongly prone to drainage.

However, it has to be pointed out that we are presently in the very beginning of hte project. Not all the samples could be analyzed yet and more low gravity experiments are needed to improve statistics.

In the future we intend to do more experiments with lead foams of lower oxide content than usual. As mentioned oxides are thought to play a major role for the process and in fact first experiments have shown a significantly enhanced tendency to drainage of this materials.

Additionally we are planning to explore the influence of acceleration to other, high acceleration side by processing samples in a centrifuge. This device will provide accelerations of up to 30g. In this case the influence of drainage is expected to dominate that of surface tension so that we are able to investigate both effects separately.

Experiments under varied surrounding conditions such as gas ambient and/or under pressure situations will give additional knowledge about the foam generation process.

7 References

[1] J. Banhart, *Metal foam: a recipe*. europhysics news, **30**, 17 (1999)

[2] H. Stanzick, J. Banhart, L. Helfen, T. Baumbach, *In-situ monitoring of metal foam evolution and decay*. 3rd Euroconference on Foams, Delft 5.-8.6.2000, MIT-Verlag Bremen (2000)

[3] G. Verbist, D. Weaire, A.M. Kraynik, *The foam drainage equation*. J. Phys. Condens. Matter **8** (1996), pp 3715-3731

[4] D. Weaire, S. Hutzler, The Physics of Foams. Oxford University Press (2000)

8 Acknowledgements

This work was supported by **DLR** (research project 50WM9821: lead foams) and by **ESA** (parabolic flight opportunity for lead foams and support via Topical Team "Foams and Capillary Flow").